# Progress in NNLO calculations for scattering processes

Nigel Glover (IPPP, Durham)

September 2002

▷ basic scattering processes like (for example)

- $pp \to$ jets,
- $ep \to 2+1$ jets,
- $e^+e^- \to 3$ jets

where the data is copious (and very precise) at LEP, TEVATRON, HERA, LHC and LC.[a]. Processes with massless internal propagators and at most one off-shell leg.

- Why go beyond NLO?
- Method - see later
- Brief survey of results
- Outlook

[a] Not single scale processes like DIS, Drell-Yan or Higgs production (see later)

# Why go beyond NLO?

In many cases, the uncertainty from the pdf's and from the choice of renormalisation scale give uncertainties that are as big or bigger than the experimental errors.

- Evolution of strong coupling constant in $p\bar{p} \rightarrow jet$

- Extracting $\alpha_s$ at each value of jet energy demonstrates running of coupling constant and gives

$$\alpha_s(M_Z) = 0.1129 \pm 0.0001(stat)^{+0.0078}_{-0.0089}(exp.syst)$$

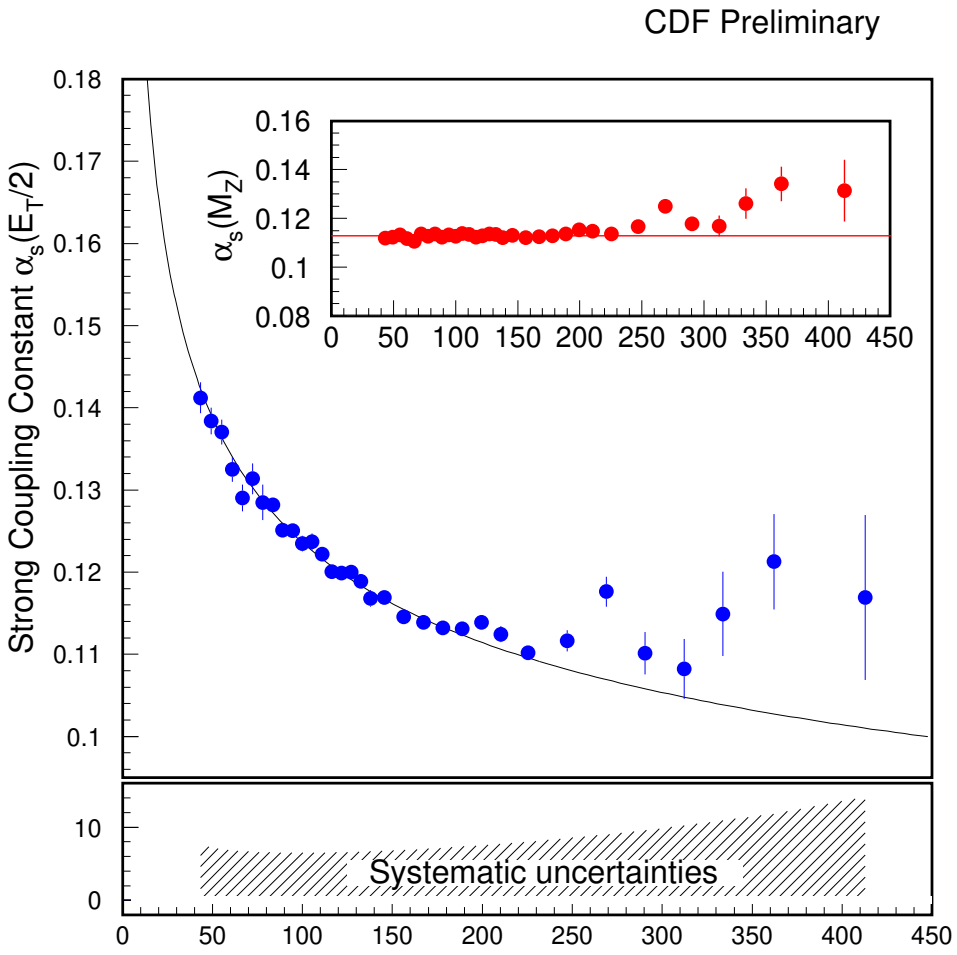

e.g. theoretical uncertainties in $\alpha_s$ extraction from $p\bar{p} \rightarrow$ jet are due to renormalisation scale and pdf's

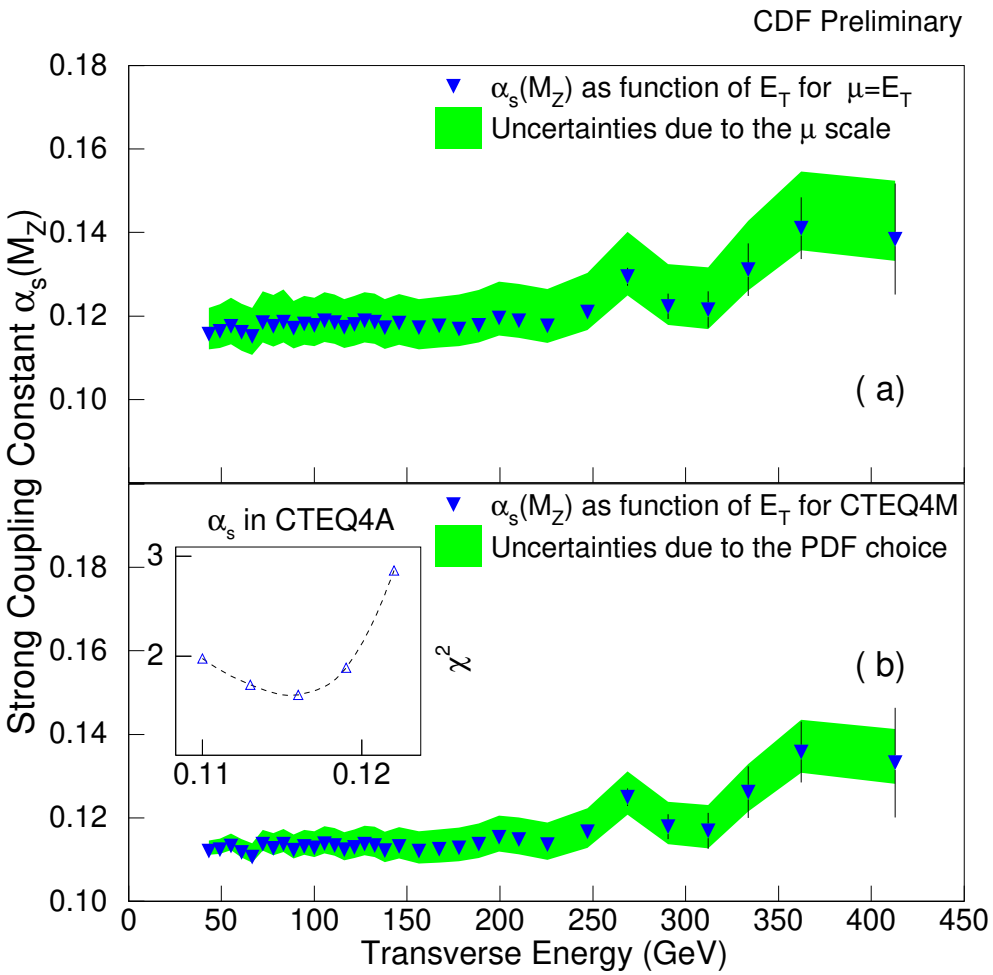

# Why do we vary renormalisation scale?

- The theoretical prediction should be independent of $\mu_R$
- The change due to varying the scale is formally higher order. If an observable $\mathcal{O}bs$ is known to order $\alpha_s^N$ then,

$$\frac{\partial}{\partial \ln(\mu_R^2)} \sum_0^N A_n(\mu_R)\alpha_s^n(\mu_R) = \mathcal{O}\left(\alpha_s^{N+1}\right).$$

- ... but the variation only produces copies of the lower order terms

  e.g.

$$\mathcal{O}bs = A_0\alpha_s(\mu_R) + \left(A_1 + b_0 A_0 \ln\left(\frac{\mu_R^2}{\mu_0^2}\right)\right)\alpha_s(\mu_R)^2$$

  $A_1$ will contain logarithms and constants that are not present in $A_0$ and therefore cannot be predicted by varying $\mu_R$.

  For example, $A_0$ may contain infrared logarithms $L$ up to $L^2$, while $A_1$ would contain these logarithms up to $L^4$.

- $\mu_R$ variation is only an estimate of higher order terms
- A large variation probably means that predictable higher order terms are large - but doesnt say anything about $A_1$.

# Renormalisation scale dependence

For example, $p\bar{p} \to$ jet, scale dependence is predictable with NLO calculation

$$\begin{aligned}\frac{d\sigma}{dE_T} &= \alpha_s^2(\mu_R)A \\ &+ \alpha_s^3(\mu_R)\left(B + 2b_0 L A\right) \\ &+ \alpha_s^4(\mu_R)\left(C + 3b_0 L B + (3b_0^2 L^2 + 2b_1 L)A\right)\end{aligned}$$

with $L = \log(\mu_R/E_T)$.

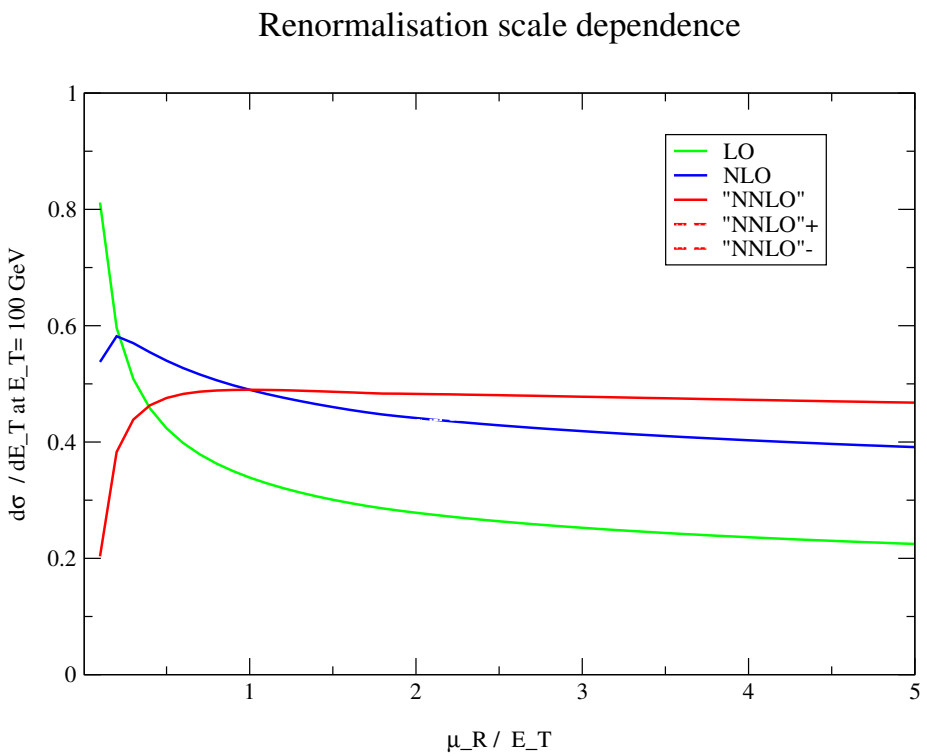


Figure 1: Single jet inclusive distribution at $E_T = 100$ GeV and $0.1 < |\eta| < 0.7$ at $\sqrt{s} = 1800$

The NNLO coefficient C is unknown. The curves show guesses $C = 0$ (solid) and $C = \pm B^2/A$ (dashed). Scale

# Renormalisation scale uncertainty

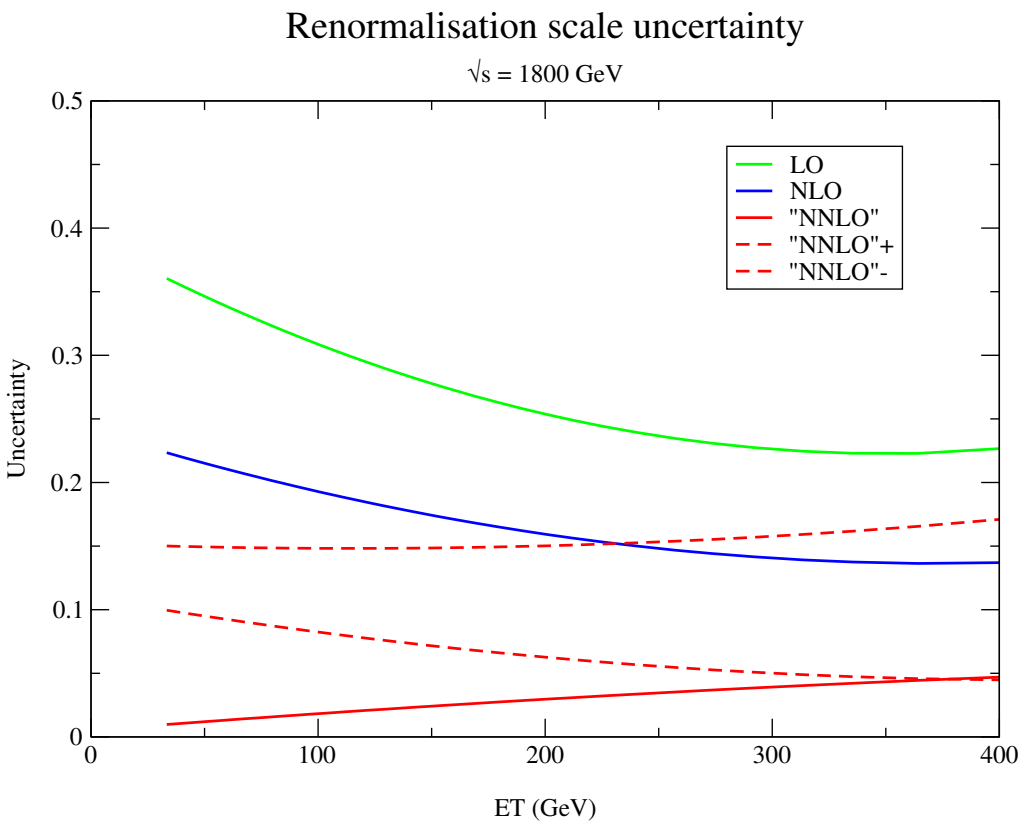


Figure 2: Uncertainty obtained by varying $\mu_R$ between $E_T/2$ and $2E_T$ (and keeping $\mu_F = E_T$).

$\Longrightarrow$ Inclusion of NNLO contribution should significantly decrease theoretical renormalisation scale uncertainty for that observable

# Jet algorithms

Also there is a mismatch between the number of hadrons and the number of partons in the event. At NLO at most two partons make a jet - while at NNLO three partons can combine to form the jet

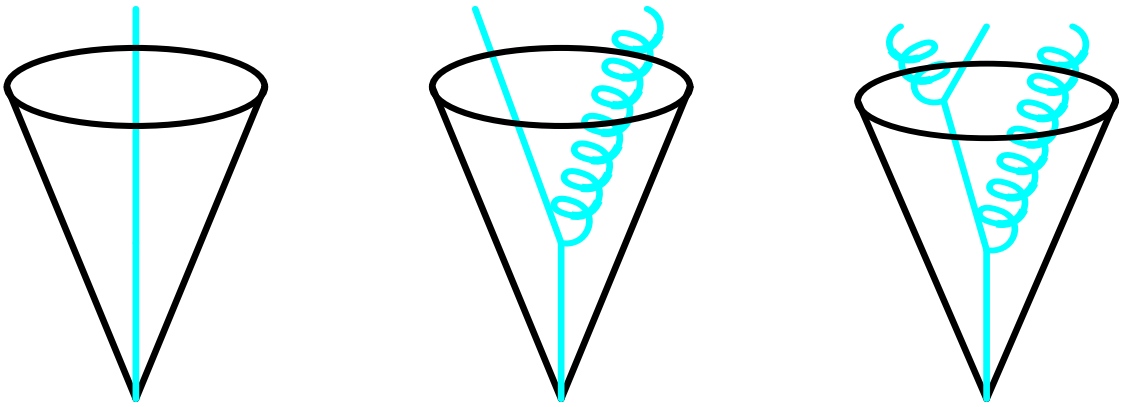

LO NLO NNLO

Perturbation theory starts to reconstruct the shower

$\Longrightarrow$ better matching of jet algorithm between theory and experiment

$\Longrightarrow$ need for better jet algorithms

# Description of the initial state

LO At lowest order final state has no transverse momentum

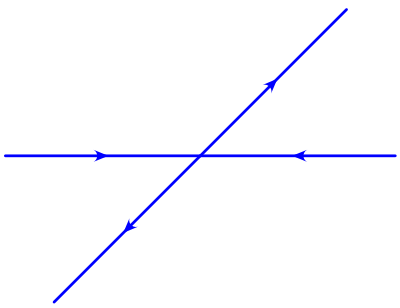

NLO Single hard radiation gives final state transverse momentum, even if no additional jet observed

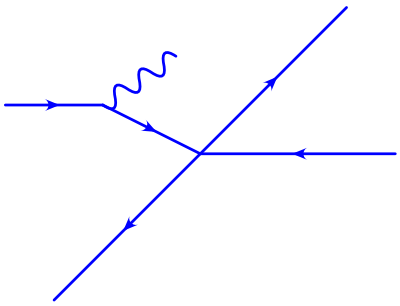

NNLO Double radiation on one side or single radiation off each incoming particle gives more complicated transverse momentum to final state

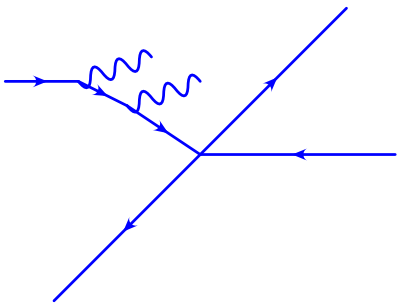

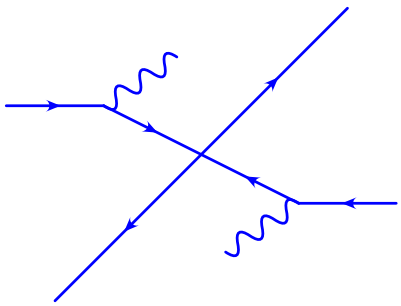

# Higher orders and power corrections

NLO Phenomenological power corrections match data with coefficient of $1/Q$ extracted from data.

$$\langle 1-T\rangle \sim 0.33\alpha_s + 1.0\alpha_s^2 + \frac{\lambda}{Q}$$

At NLO, $\lambda \sim 1$ GeV gives a good description of the data.

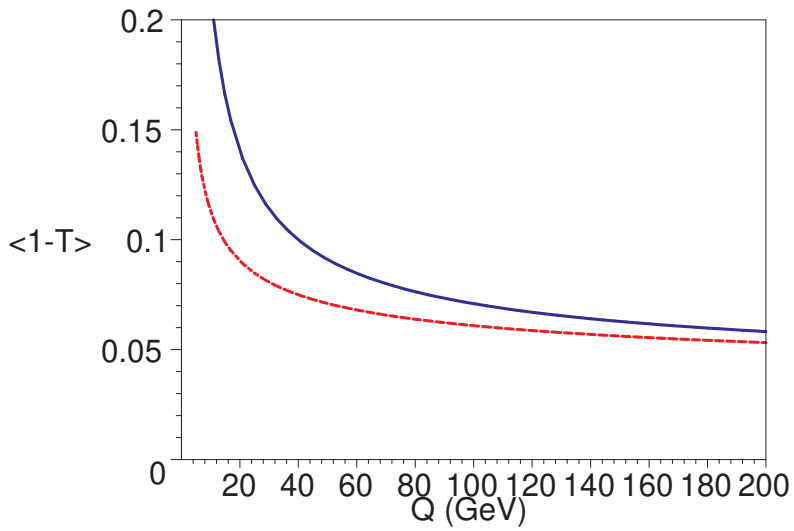


Figure 3: .$\langle 1-T\rangle$ with NLO and no power correction and NLO with power correction $\lambda = 1$ GeV.

The power correction parameterises the unknown higher orders as well as the genuine non-perturbative correction

# Higher orders or power corrections

NNLO Higher orders partially remove need for power correction

$$\langle 1 - T \rangle \sim 0.33\alpha_s + 1.0\alpha_s^2 + A\alpha_s^3 + \frac{\lambda \text{ GeV}}{Q}$$

If we guess $A = 3$, then $\lambda = 0.5$ GeV is good fit.

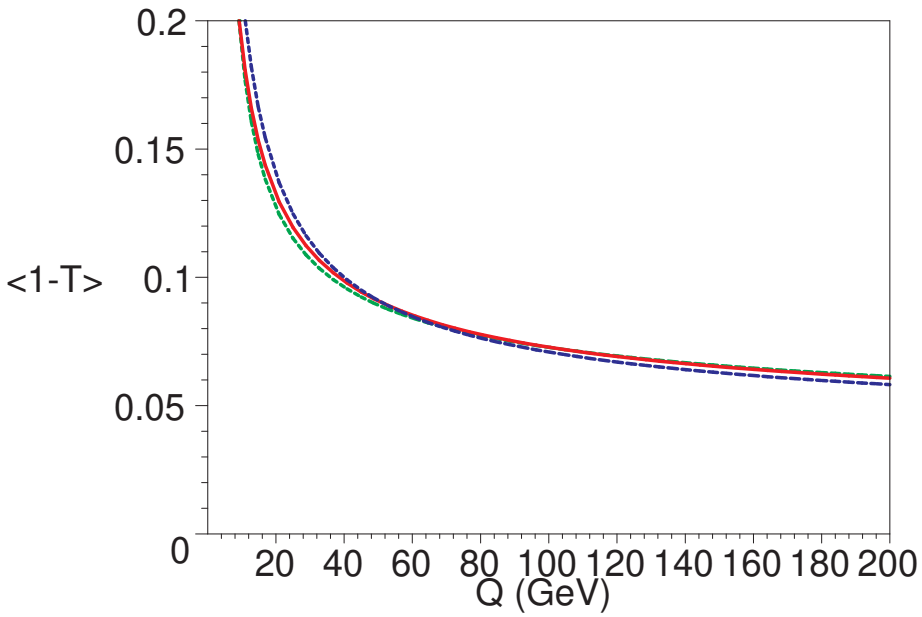


Figure 4: $\langle 1-T \rangle$ with NLO and $\lambda = 1$ GeV, "NNLO" with $\lambda = 0.5$ GeV and "All orders" with no power correction.

At present data not good enough to tell difference between $1/Q$ and $1/\log(Q/\Lambda)^3$.

All orders If higher orders form geometric series, then can avoid power correction altogether!!

# Why go beyond NLO? - summary

We expect a variety of improvements at NNLO

- $\surd$ Reduced renormalisation scale dependence
- $\surd$ Better matching of parton-level jet algorithm with experimental hadron-level algorithm
- $\surd$ Better description of transverse momentum of final state due to double radiation of initial state
- $\surd$ Reduced power correction as higher perturbative powers of $1/\ln(Q/\Lambda)$ mimic genuine power corrections like $1/Q$.
- $\surd$ Full NNLO global fit of PDF's should also reduce the theoretical uncertainty
- $\surd$ ...

These improvements will be necessary if and when the experimental accuracy for a given observable is better than the 10% level.

# Multiparticle production: NNLO

Example, pure gluon ingredients to $pp \longrightarrow 2$ jets

- 2 loop, 2 parton final state

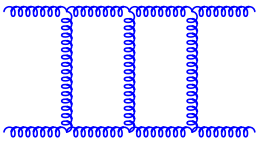

- $|$ 1 loop $|^2$, 2 parton final state

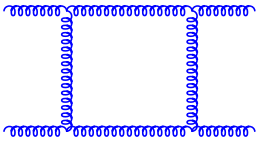

- 1 loop, 3 parton final states
  or 2+1 parton final state

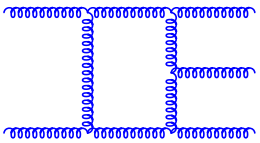

- tree, 4 parton final states
  or 3+1 parton final states
  or 2+2 parton final state

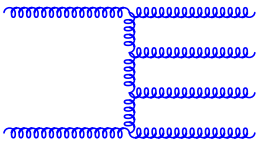

where n theoretically unresolved soft or collinear partons are indicated as +n

▷ Much more sophisticated infrared cancellation between

- $n$ and $n+1$ particle contributions when one particle unresolved
  $\Longrightarrow$ soft and collinear limits of one loop amplitudes
- $n$ and $n+2$ particle contributions when two particles unresolved

▷ For now focus on two-loop contributions.

# Two-loop matrix elements for scattering processes

| On-shell Process | Tree $\times$ Two-loop | Helicity amplitudes |
|---|---|---|
| $e^+e^- \to \mu^+\mu^-(e^+e^-)$ | $\surd$(00) | |
| $q\bar{q} \to q\bar{q}(\bar{q}'q')$ | $\surd$(00) | |
| $q\bar{q} \to gg$ | $\surd$(01) | |
| $gg \to gg$ | $\surd$(01) | $\surd$(00), $\overline{\surd}$(02) |
| $gg \to \gamma\gamma$ | — | $\surd$(01) |
| $\gamma\gamma \to \gamma\gamma$ | — | $\surd$(01), $\overline{\surd}$(02) |
| $q\bar{q} \to g\gamma(\gamma\gamma)$ | $\surd$(02) | |
| Off-shell Process | | |
| $e^+e^- \to q\bar{q}g$ | $\surd\surd$(01) | $\surd\surd$(02), $\surd$(02) |

$\surd$ Bern, De Freitas, Dixon, Ghinculov, Kosower, Wong

$\surd$ Anastasiou, Binoth, Glover, Marquard, Oleari, Tejeda-Yeomans, van der Bij

$\surd\surd$ Garland, Gehrmann, Glover, Koukoutsakis, Remiddi

$\surd$ Moch, Uwer, Weinzierl

Rapid progress in last two years...since Loops and Legs in Bastei

# On-shell Master Integrals

- The trivial topologies

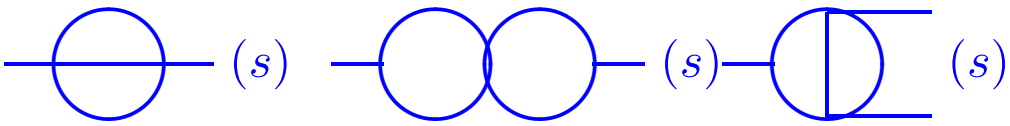


- The less trivial topologies

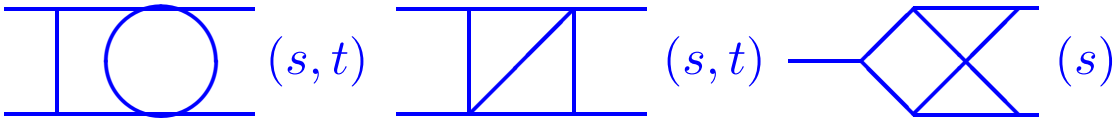


- The non-trivial topologies
  - ▷ The planar boxes

Smirnov, hep-ph/9905323

Smirnov and Veretin, hep-ph/9907385

  - ▷ The non-planar boxes

Tausk, hep-ph/9909506

Anastasiou, Gehrmann, Oleari, Remiddi and Tausk, hep-ph/0003261

# Master Integrals - one offshell leg

- Much more complicated and require new (2-dimensional harmonic polylogarithm) functions to describe them
- there are also many more

Gehrmann and Remiddi, hep-ph/0008287, hep-ph/0101124

For example,

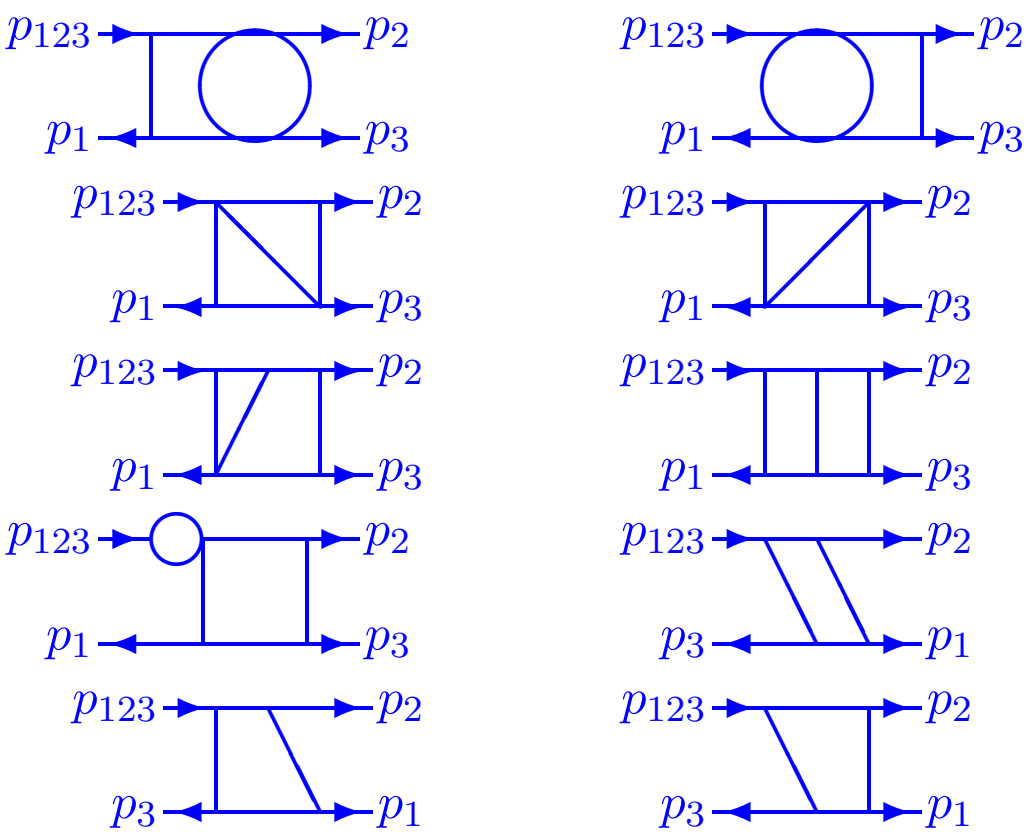


plus five extra integrals needed for the tensors.

# Example series expansion

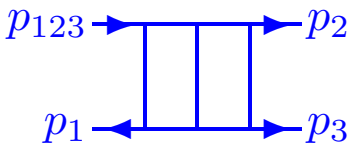


$$= \left(\frac{S_\epsilon}{16\pi^2}\right)^2 \frac{(-s_{123})^{-2\epsilon}}{s_{13}s_{23}^2} \sum_{i=0}^{4} \frac{f_{7.1,i}\left(\frac{s_{13}}{s_{123}}, \frac{s_{23}}{s_{123}}\right)}{\epsilon^i}$$

$$f_{7.1,4}(y,z) = -1 \ ,$$

$$f_{7.1,3}(y,z) = 2\left[H(0;y) + H(0;z)\right] \ ,$$

$$f_{7.1,2}(y,z) = -4H(0;y)H(0;z) - 4H(0,0;y) - 4H(0,0;z) - H(1,0;y) - 3H(1,0;z) - \frac{7\pi^2}{12} \ ,$$

$$\begin{aligned}
f_{7.1,1}(y,z) = {} & +6H(0;y)H(1,0;z) + 2H(0;z)H(1-z,0;y) + 8H(0,0;y)H(0;z) \\
& +8H(0,0;z)H(0;y) + 8H(0,0,0;y) + 8H(0,0,0;z) + 5H(0,1,0;y) \\
& +6H(0,1,0;z) + 2H(1,0;z)H(1-z;y) + 2H(1,0,0;y) + 9H(1,0,0;z) \\
& -2H(1,1,0;y) + 6H(1,1,0;z) + 2H(1-z,1,0;y) - \frac{\zeta_3}{2} \\
& +\frac{\pi^2}{6}\left[+7H(0;y) + 7H(0;z) - 2H(1;y) + 6H(1;z) + 2H(1-z;y)\right] \ ,
\end{aligned}$$

$$\begin{aligned}
f_{7.1,0}(y,z) = {} & -18H(0;y)H(1,0,0;z) - 12H(0;y)H(1,1,0;z) + 2H(0;z)H(1,1-z,0;y) \\
& -4H(0;z)H(1-z,0,0;y) - 2H(0;z)H(1-z,1-z,0;y) - 16H(0,0;y)H(0,0;z) \\
& -12H(0,0;y)H(1,0;z) + 2H(0,0;z)H(1,0;y) - 6H(0,0;z)H(1-z,0;y) \\
& -16H(0,0,0;y)H(0;z) - 16H(0,0,0;z)H(0;y) - 16H(0,0,0,0;y) \\
& -16H(0,0,0,0;z) - 16H(0,0,1,0;y) - 12H(0,0,1,0;z) - 12H(0,1,0;z)H(0;y) \\
& +2H(0,1,0;z)H(1;y) - 6H(0,1,0;z)H(1-z;y) - 10H(0,1,0,0;y) \\
& -18H(0,1,0,0;z) + H(0,1,1,0;y) - 12H(0,1,1,0;z) - 10H(0,1-z;y)H(1,0;z) \\
& -10H(0,1-z,0;y)H(0;z) - 10H(0,1-z,1,0;y) + 2H(1,0;y)H(1,0;z) \\
& +2H(1,0;z)H(1,1-z;y) - 4H(1,0;z)H(1-z,0;y) - 2H(1,0;z)H(1-z,1-z;y \\
& -6H(1,0,0;z)H(1-z;y) - 4H(1,0,0,0;y) - 21H(1,0,0,0;z) - 2H(1,0,1,0;y) \\
& -15H(1,0,1,0;z) + 2H(1,1,0;z)H(1;y) - 4H(1,1,0;z)H(1-z;y) \\
& +4H(1,1,0,0;y) - 21H(1,1,0,0;z) - 4H(1,1,1,0;y) - 12H(1,1,1,0;z) \\
& +2H(1,1-z,1,0;y) - 2H(1-z,0,1,0;y) - 4H(1-z,1,0,0;y) \\
& +4H(1-z,1,1,0;y) - 2H(1-z,1-z,1,0;y) - \frac{\pi^4}{4} \\
& +\zeta_3\left[+H(0;y) - 2H(1-z;y) - 6H(1;y) + 3H(1;z) + H(0;z)\right] \\
& +\frac{\pi^2}{6}\Big[ -14H(0;y)H(0;z) - 12H(0;y)H(1;z) + 2H(0;z)H(1;y) - 2H(0;z)H(1- \\
& -14H(0,0;y) - 14H(0,0;z) + H(0,1;y) - 12H(0,1;z) - 10H(0,1-z;y) \\
& +2H(1;y)H(1;z) - 4H(1;z)H(1-z;y) - 15H(1,0;z) - 4H(1,1;y) - 12H(1,1;z) \\
& +2H(1,1-z;y) - 4H(1-z,0;y) + 4H(1-z,1;y) - 2H(1-z,1-z;y)\Big] \ .
\end{aligned}$$

# Checks of results

- Infrared singularity structure Catani, hep-ph/9802439

$$|\mathcal{M}^{(2)}\rangle = \boldsymbol{I}^{(1)}(\epsilon)\,|\mathcal{M}^{(1)}\rangle + \boldsymbol{I}^{(2)}(\epsilon)\,|\mathcal{M}^{(0)}\rangle + |\mathcal{M}^{(2)\,\mathrm{fin}}\rangle$$

▷ first term: the process dependent but predictable one-loop insertion operator $\boldsymbol{I}^{(1)}$ acts onto one-loop matrix element

▷ second term: new colour-charge operator $\boldsymbol{I}^{(2)}$ acts onto tree-level matrix element,

$$\begin{aligned}\boldsymbol{I}^{(2)}(\epsilon) \;=\; & -\frac{1}{2}\boldsymbol{I}^{(1)}(\epsilon)\left(\boldsymbol{I}^{(1)}(\epsilon)+\frac{2\beta_0}{\epsilon}\right) \\ & +e^{-\epsilon\gamma}\frac{\Gamma(1-2\epsilon)}{\Gamma(1-\epsilon)}\left(\frac{\beta_0}{\epsilon}+K\right)\boldsymbol{I}^{(1)}(2\epsilon)+\boldsymbol{H}^{(2)}\end{aligned}$$

▷ The function $\boldsymbol{H}^{(2)}$ contains only single poles and is process and scheme dependent.

- High energy limit :

in the $t \to 0$ limit, the parton-parton scattering amplitudes should reproduce the $\log(-s/t)$ structure resummed by the BFKL equation.

# Infrared singularity structure cont

Catani, hep-ph/9802439

- pole structure of two-loop amplitude interfered with tree-level

$$\begin{aligned}\mathcal{P}oles = 2\,\mathrm{Re}\Bigg[ & \frac{1}{2}\langle\mathcal{M}^{(0)}|\boldsymbol{I}^{(1)}(\epsilon)\boldsymbol{I}^{(1)}(\epsilon)|\mathcal{M}^{(0)}\rangle \\ & + \langle\mathcal{M}^{(0)}|\boldsymbol{I}^{(1)}(\epsilon)|\mathcal{M}^{(1)\,fin}\rangle - \frac{\beta_0}{\epsilon}\,\langle\mathcal{M}^{(0)}|\boldsymbol{I}^{(1)}(\epsilon)|\mathcal{M}^{(0)}\rangle \\ & + e^{-\epsilon\gamma}\,\frac{\Gamma(1-2\epsilon)}{\Gamma(1-\epsilon)}\left(\frac{\beta_0}{\epsilon}+K\right)\langle\mathcal{M}^{(0)}|\boldsymbol{I}^{(1)}(2\epsilon)|\mathcal{M}^{(0)}\rangle \\ & + \langle\mathcal{M}^{(0)}|\boldsymbol{H}^{(2)}(\epsilon)|\mathcal{M}^{(0)}\rangle\Bigg]\end{aligned}$$

- The finite remainder is defined as

$$\mathcal{F}inite = 2\,\mathrm{Re}\langle\mathcal{M}^{(0)}|\mathcal{M}^{(2)}\rangle - \mathcal{P}oles$$

and is typically given in terms of real logs and polylogs for each scattering channel and each colour

# Finite parts

e.g., leading colour part of $q_1\bar{q}_1 \longrightarrow q_2\bar{q}_2$

$$
\begin{aligned}
A_s \quad = \quad & \left[ 2\,\mathrm{Li}_4(x) + \left( -2\,X - \frac{11}{3} \right) \mathrm{Li}_3(x) + \left( X^2 + \frac{11}{3}\,X - \frac{2}{3}\,\pi^2 \right) \mathrm{Li}_2(x) \right. \\
& + \frac{121}{18}\,S^2 + \left( -\frac{11}{3}\,X^2 + 11\,X - \frac{296}{27} \right) S + \frac{1}{6}\,X^4 + \left( \frac{1}{3}\,Y - \frac{49}{18} \right) X^3 \\
& + \left( \frac{11}{6}\,Y - \frac{5}{6}\,\pi^2 + \frac{197}{18} \right) X^2 + \left( -\frac{2}{3}\,Y\,\pi^2 - \frac{47}{18}\,\pi^2 + 6\,\zeta_3 - \frac{95}{24} \right) X \\
& \left. + \left( \frac{11}{24}\,\pi^2 - 7\,\zeta_3 - \frac{409}{216} \right) Y + \frac{113}{720}\,\pi^4 - \frac{7}{6}\,\pi^2 + \frac{197}{36}\,\zeta_3 + \frac{23213}{2592} \right] \left[ \frac{t^2+u^2}{s^2} \right] \\
& + \left[ -3\,\mathrm{Li}_4(y) + 6\,\mathrm{Li}_4(x) - 3\,\mathrm{Li}_4(z) + \left( -2\,X - \frac{7}{2} \right) \mathrm{Li}_3(x) \right. \\
& + 3\,X\,\mathrm{Li}_3(y) + \left( \frac{1}{2}\,X^2 + \frac{7}{2}\,X + \frac{1}{2}\,\pi^2 \right) \mathrm{Li}_2(x) + \left( -\frac{11}{6}\,X^2 + \frac{11}{6}\,X \right) S \\
& + \left( \frac{1}{2}\,Y\,\pi^2 - \frac{13}{9}\,\pi^2 - \zeta_3 - \frac{32}{9} \right) X + \left( \frac{7}{4}\,Y - \frac{3}{4}\,\pi^2 + \frac{44}{9} \right) X^2 \\
& \left. + \left( \frac{1}{2}\,Y - \frac{49}{36} \right) X^3 - \frac{7}{120}\,\pi^4 + \frac{47}{36}\,\pi^2 + 2\,\zeta_3 \right] \left[ \frac{t^2-u^2}{s^2} \right] + \left[ 3\,X^2 \right] \frac{t^3}{s^2 u} \\
& + 3\,\mathrm{Li}_4(y) - 3\,\mathrm{Li}_4(x) + 3\,\mathrm{Li}_4(z) - 3\,X\,\mathrm{Li}_3(y) - \frac{5}{2}\,\mathrm{Li}_3(x) \\
& + \left( \frac{5}{2}\,X - \frac{1}{2}\,\pi^2 \right) \mathrm{Li}_2(x) - \frac{11}{6}\,X\,S + \frac{1}{8}\,X^4 + \left( -\frac{1}{2}\,Y + \frac{1}{3} \right) X^3 \\
& + \left( \frac{5}{4}\,Y + \frac{1}{4}\,\pi^2 + \frac{1}{6} \right) X^2 + \left( -\frac{1}{2}\,Y\,\pi^2 - \frac{7}{6}\,\pi^2 + 3\,\zeta_3 + \frac{32}{9} \right) X \\
& + \frac{1}{40}\,\pi^4 - \frac{11}{36}\,\pi^2 + 4\,\zeta_3
\end{aligned}
$$

$$x = -\frac{t}{s}, \quad y = -\frac{u}{s}, \quad X = \ln(x), \quad Y = \ln(y), \quad S = \ln\left(\frac{s}{\mu^2}\right)$$

# Conclusions

- ▷ Many $2 \to 2$ scattering processes with up to one off-shell leg now calculated at two-loops
  - $\surd$ strong checks with infrared pole structure, high energy limit, QED results
  - $\surd$ form a crucial part of the NNLO predictions for jet cross sections at LEP, HERA, TEVATRON, LHC, LC...
  - $\surd$ must be combined with the tree-level $2 \to 4$, the one-loop $2 \to 3$ and the self-interference of the one-loop $2 \to 2$ to yield physical cross sections
  - — this is still some way away but lots of ideas and expect progress very soon – see talks later in the workshop
- ▷ Together with NNLO DIS, Drell-Yan and the exact calculations of the splitting functions, the NNLO $p\bar{p} \to$ jet cross section will make form a global set of NNLO variables that can test QCD over a wide range of energies
- ▷ The NNLO $e^+e^- \to 3$ jet cross section should allow a measurement of $\alpha_s(M_Z)$ at the 1% level.
- ▷ There are many other interesting processes worth calculationg at NNLO, such as $p\bar{p} \to b\bar{b}$ that require the evaluation of more two-loop master integrals.